



Cite this: *Green Chem.*, 2021, **23**, 9800

# Production of chemicals from marine biomass catalysed by acidic ionic liquids

Li Liu <sup>a,b</sup>

The past decade has witnessed the rapid development of shell biorefining. Among the green methodologies, the application of ionic liquids (ILs) to catalyze the conversion of marine biomass including chitosan, chitin, and crustacean shells, has attracted increasing attention. However, in comparison with the significant achievements of ILs in the conversion of lignocellulosic biomass, the methodological developments of ILs in marine biomass have been rather limited due to the greater structural complexity of marine biomass. Herein, the conversion of marine biomass to a variety of value-added chemicals (chitosan oligomers, sugars, 3-acetamido-5-acetylfuran, 5-hydroxyfurfural, levulinic acid, etc.) using acidic ILs as catalysts, has been reviewed according to the order of feedstock from simple to complex (chitosan, chitin, and crustacean shells). The different characteristics of ILs for each type of marine biomass have been summarized and compared with lignocellulosic biomass for the first time, with respect to acidity, hydrogen bonding ability and recyclability, demonstrating the structural effect of marine biomass on their conversion.

Received 6th September 2021,

Accepted 1st November 2021

DOI: 10.1039/d1gc03249f

rsc.li/greenchem

## 1. Introduction

Relative to the remarkable achievements in lignocellulosic biorefinery,<sup>1–19</sup> the conversion of marine biomass, especially crustacean shells, has a rather short history. Globally, 6–8 million tons of crab and shrimp shells are discarded every year,<sup>20</sup> causing serious resource waste and environmental pollution. Over the long term, converting the shell resources efficiently into high value-added chemicals can not only promote the circular economy but also help to protect the environment.<sup>21–33</sup> However, less than 2.5% of about 30 000 publications on renewable biomass concentrated on crustacean shells suggests great potential to utilize crustacean shells for chemical production.

Crustacean shells are mainly composed of chitin (15–40%), protein (20–40%), and calcium carbonate (20–50%), of which chitin is the second largest biomass in the world next to cellulose.<sup>33</sup> Chitin is structurally similar to cellulose and has an acetamide group at the C-2 position instead of the hydroxyl group as in cellulose. Chitosan is a deacetylative derivative of chitin and has more similarities with cellulose. The only difference also depends on the functional group at the C-2 position, i.e., amino group for chitosan and hydroxyl group for cellulose.

Due to a lack of mechanistic understanding, the methodologies to convert chitin and chitosan have lagged far behind in comparison with that of cellulose. Certainly, whether the

<sup>a</sup>College of Chemistry and Chemical Engineering, Inner Mongolia University, Hohhot 010020, China. E-mail: lliu@imu.edu.cn

<sup>b</sup>Fujian Provincial Key Lab of Coastal Basin Environment, Fujian Polytechnic Normal University, Fuzhou 350300, China



Li Liu

*Dr Li Liu obtained her bachelor's degree from Nankai University in 1998 and completed her Ph.D. at Shanghai Institute of Organic Chemistry, CAS in 2003. After postdoctoral research at Portland State University (USA) and University of Cambridge (UK), she joined Dalian Institute of Chemical Physics, CAS as an associate professor and DICP-100-Talents in 2008. She moved to Dalian University of Technology in 2013, and since*

*2021 she has been a group leader at the Inner Mongolia University supported by the Program of Higher-Level Talents. Her research interests include biomass utilization, ionic liquids, supramolecular chemistry and nanotechnology.*

feedstock contains nitrogen or not can make a big difference. On the one hand, owing to the advantage of containing nitrogen in chitin and chitosan feedstocks, the nitrogen could be passed on to the chemical product in the absence of any other nitrogen source, which is impossible for cellulose.<sup>34</sup> On the other hand, the existence of the amino group in chitosan or the acetamide group in chitin results in different mechanisms than in cellulose, which have not been thoroughly elucidated in the previous studies.

Ionic liquids (ILs) have been widely used in green chemistry, due to their characteristics of designability and recyclability.<sup>35–37</sup> Application of ILs has greatly contributed to the development of lignocellulosic biorefining,<sup>5,38–48</sup> since Rogers' group first reported dissolving cellulose in [C<sub>4</sub>mim]Cl in 2002,<sup>38</sup> which profoundly inspired their applications in the field of marine biomass. In 2006, Xie and Zhang<sup>49</sup> found that [C<sub>4</sub>mim]Cl could also be utilized to dissolve chitosan and chitin. Thereafter, Wu *et al.*<sup>50</sup> proposed [C<sub>4</sub>mim]OAc to be a better solvent for chitosan and chitin. Rogers *et al.*<sup>51</sup> adopted [C<sub>2</sub>mim]OAc to dissolve raw crustacean shells, which exhibited higher solubility than [C<sub>4</sub>mim]Cl and [C<sub>2</sub>mim]Cl. Likewise, applications of ILs to dissolve chitosan, chitin, and crustacean shells have led to some progress in derivatization and functionalization.<sup>52,53</sup>

Early interest in utilizing ILs for the production of chemicals from marine biomass was focused on the solvent role. For example, Zhao *et al.* reported the conversion of chitosan and chitin in [C<sub>4</sub>mim]Cl/Br using mineral acid catalysts, leading to higher total reducing sugar (TRS) yields when compared with water-involving processes.<sup>54</sup> These methods illustrated that IL solvents are oftentimes advantageous to facilitate the hydrolysis of chitosan and chitin. On the other hand, the IL solvent systems have some shortcomings, such as the lack of control of the strength of the acidic catalysts, leading to low selectivity due to further degradation of the products into unwanted chemicals. Correspondingly, ILs can provide a solution to this problem by incorporating the acid functionality into either the cation or anion, whereby the strength of the acidic ILs can be modulated by the design of the IL structures.<sup>62</sup> At present, the production of chemicals from marine biomass, including chitosan, chitin, and crustacean shells using acidic ILs as catalysts has just started.

In this review, the chemical routes from crustacean shells to chitin, chitosan, oligomers, sugars, 3-acetamido-5-acetylfuran (3A5AF), 5-hydroxyfurfural (HMF), and levulinic acid (LA) have been outlined (Fig. 1). The relevant literature using acidic ILs as catalysts to convert chitosan, chitin and crustacean shells to oligomers, sugars, 3A5AF, HMF and LA have been listed in Table 1. Firstly, according to the order of feedstock from simple to complex, the eminent research using acidic ILs to convert chitosan, chitin, and crustacean shells to downstream chemicals will be summarized in turn. The IL structures reported in the literature will be discussed in detail as well (Fig. 2). Secondly, the recyclability of ILs for these three types of marine biomass, including chitosan, chitin, and crustacean shells will be reviewed.

## 2. Conversion of chitosan to chemicals catalysed by ILs

By virtue of the amino groups, the hydrogen bonding in chitosan is stronger than in cellulose, resulting in its notorious resistance to dissolution. Applications of ILs in chitosan research started from early interest in chitosan dissolution,<sup>27,49,50,65</sup> to chitosan conversion in IL solvents.<sup>54</sup> Zhao and co-workers<sup>54</sup> used [C<sub>4</sub>mim]Cl or [C<sub>4</sub>mim]Br as the solvent and mineral acids (HCl, HNO<sub>3</sub>, and H<sub>2</sub>SO<sub>4</sub>) as the catalyst to hydrolyze chitosan into TRS of 63%. Recently, Zang and co-workers<sup>66</sup> reported that 44.1 mol% HMF could be obtained from chitosan using Brønsted–Lewis acidic ILs ([Hmim]HSO<sub>4</sub>–0.5FeCl<sub>2</sub>) as catalysts. We explored the selective conversion of chitosan to LA (64%) catalysed by ILs,<sup>61</sup> on the basis of our previous research on IL-catalysed conversions of cellulose<sup>45,67</sup> and lignocellulose,<sup>68</sup> thus revealing the effect of the –NH<sub>2</sub> group on chitosan conversion.

### 2.1 Chitosan oligomers

Chitosan with high molecular weight ( $M_w$ ) has some shortcomings that hinder its practical usage, such as poor solubility and low bulk density. Hence, it is necessary to reduce the  $M_w$  of chitosan to enhance the solubility, so as to enlarge its application scope. Moreover, good water solubility could endow chitosan oligomers with some special physiological properties towards applications in cosmetics and health, *e.g.*, antifungal, antibacterial, and antitumor effects. Chitosan oligomers can be prepared by different methods including enzymatic hydrolysis, oxidative hydrolysis and acid hydrolysis.<sup>56</sup>

Shan and co-workers<sup>69</sup> established oxidative hydrolysis of chitosan with molecular oxygen as the oxidant catalyzed by iron(II) phthalocyanine (FePc) in [C<sub>4</sub>mim]NTf<sub>2</sub> (1-methyl-3-butylimidazolium bis((trifluoromethyl)sulfonyl)imide) to form chitosan oligomers in a biphasic system. When the temperature was increased from 40 °C to 120 °C for 6 h, the intrinsic viscosity kept decreasing. The optimal temperature was determined to be 110 °C, beyond which more complicated by-products were formed. Later, Yu *et al.*<sup>70</sup> came up with another oxidative hydrolysis system of H<sub>2</sub>O<sub>2</sub>/[Gly]Cl (glycine chloride), forming chitosan oligomers homogeneously at 80 °C for 2 h.

Conventionally, acid hydrolysis using mineral acids such as HCl and HNO<sub>3</sub> leads to the rapid and stochastic breakdown of chitosan. In order to control the  $M_w$  of the chitosan oligomer products, new techniques are required. Dandekar and co-workers<sup>55</sup> applied three SO<sub>3</sub>H-functionalized ILs (SFILs) to hydrolyze chitosan homogeneously (Table 1, entry 1). Besides [C<sub>3</sub>SO<sub>3</sub>Hmim]Cl, they designed two new ILs with Cl<sup>–</sup> as the anion, introducing the carboxymethyl group into SO<sub>3</sub>H-functionalized imidazole and benzimidazole based cationic structures, whereas the carboxymethyl groups serve as proton donors together with SO<sub>3</sub>H moieties. It has been reported that the imidazole and benzimidazole ring structures cause some differences in acidity. Therefore, three ILs with different acidities were employed for chitosan hydrolysis.

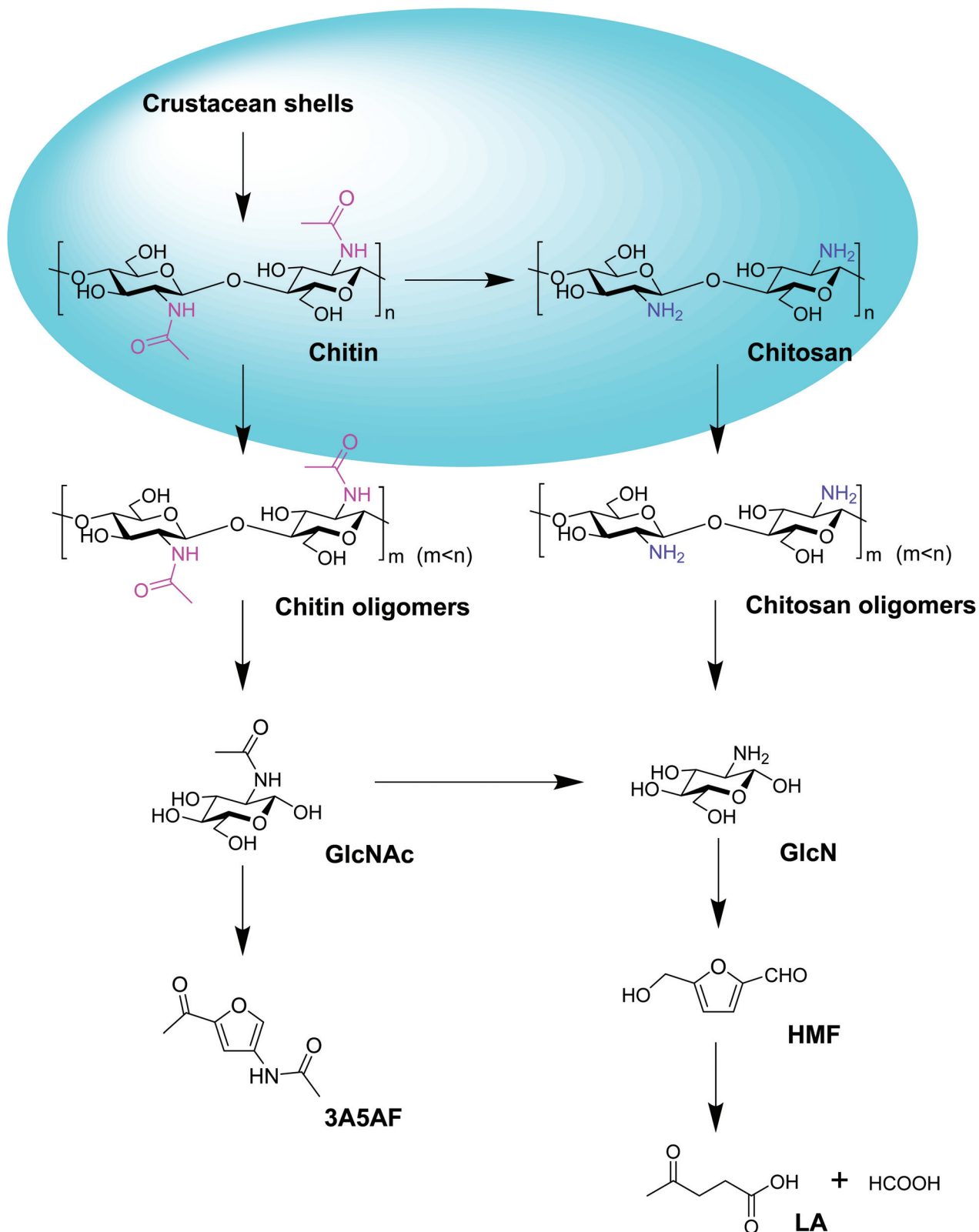


Fig. 1 Conversion of crustacean shells, chitin and chitosan to downstream chemicals.

**Table 1** Conversion of chitosan, chitin, and crustacean shells catalysed by acidic ILs

Entry	Feedstock	IL catalyst (wt%)	Solvent	Role of IL	<i>T</i> (°C)	Time	Product (yield)	Ref.
1	Chitosan	[C <sub>3</sub> SO <sub>3</sub> HCH <sub>2</sub> COOHbim]Cl (17 wt%)	H <sub>2</sub> O	Cat.	110	12 h	Chitosan oligomers (–)	55
2	Chitosan	[C <sub>3</sub> SO <sub>3</sub> HPy]HSO <sub>4</sub> (14 wt%)	[Amim]Cl–[Hmim]Cl	Cat./sol.	MW 640 W	2 min	TRS (93.2%)	56
3	Chitosan	[Hmim]HSO <sub>4</sub> (4 wt%)	H <sub>2</sub> O	Cat.	180	5 h	HMF (29.5%)	57
4	Chitosan	[Hmim]HSO <sub>4</sub> (10 wt%)	DMSO–H <sub>2</sub> O	Cat.	180	6 h	HMF (34.7%)	58
5	Chitosan	[Hmim]HSO <sub>4</sub> –0.5FeCl <sub>2</sub> (1.25 wt%)	H <sub>2</sub> O	Cat.	180	4 h	HMF (44.1%)	59
6	Chitosan	[Hbim]Cl (2.5 wt%)	DMSO–H <sub>2</sub> O	Cat.	180	3 h	HMF (34.9%)	60
7	Chitosan	[C <sub>3</sub> SO <sub>3</sub> Hmim]HSO <sub>4</sub> (20 wt%)	H <sub>2</sub> O	Cat.	170	5 h	LA (64.0%)	61
8	Chitin	[C <sub>3</sub> SO <sub>3</sub> Hmim]OTf (6 wt%)	[C <sub>4</sub> mim]Cl	Cat./sol.	120	5 h	GlcNAc (15%)	62
9	Chitin	[Hmim]HSO <sub>4</sub> (4 wt%)	H <sub>2</sub> O	Cat.	180	5 h	HMF (19.3%)	57
10	Chitin	[Hmim]HSO <sub>4</sub> (10 wt%)	DMSO–H <sub>2</sub> O	Cat.	180	6 h	HMF (25.7%)	58
11	Chitin	[C <sub>3</sub> SO <sub>3</sub> Hmim]HSO <sub>4</sub> (14 wt%)	H <sub>2</sub> O	Cat.	180	5 h	LA (67.0%)	63
12	Crab shells	[C <sub>3</sub> SO <sub>3</sub> Hmim]HSO <sub>4</sub> (20wt%)	H <sub>2</sub> O	Cat.	180	5 h	LA (77.9%)	64

After heating at 110 °C for 12 h, HCl and HOAc reduced the  $M_w$  of chitosan from 410 kDa to 14 kDa and 32 kDa, respectively. The  $M_w$  reduction of chitosan was achieved in the sequence  $\text{HCl} > [\text{C}_3\text{SO}_3\text{HCH}_2\text{COOHbim}]\text{Cl} > [\text{C}_3\text{SO}_3\text{HCH}_2\text{COOHim}]\text{Cl} > [\text{C}_3\text{SO}_3\text{Hmim}]\text{Cl} > \text{HOAc}$ , which was consistent with their acidity. Among the ILs,  $[\text{C}_3\text{SO}_3\text{HCH}_2\text{COOHbim}]\text{Cl}$  exhibited higher efficiency and reduced the  $M_w$  of chitosan to 20 kDa. It was proposed that due to the bulky character, the ILs are unable to interact with chitosan as efficiently as with mineral acids, resulting in a controlled degradation rate. Thus, ILs provided an alternative technique to produce chitosan oligomers with specific  $M_w$ .

## 2.2 TRS

Wu and co-workers<sup>56</sup> dissolved chitosan in mixed ILs of  $[\text{Amim}]\text{Cl}/[\text{Hmim}]\text{Cl}$ , and homogeneous hydrolysis quickly occurred under microwave (MW) irradiation using pyridinium-type SFILs at 640 W for 2 min (Table 1, entry 2). Noticeably, the TRS yield was improved sharply after the addition of DMSO, due to the decreased viscosity, which in turn increased the contact between  $\text{H}^+$  and the 1,4- $\beta$ -glycosidic bonds. The Brønsted acidities of the SFILs depend on the anions and decrease in the order:  $[\text{C}_3\text{SO}_3\text{HPy}]\text{HSO}_4 > [\text{C}_3\text{SO}_3\text{HPy}]\text{pTSA} > [\text{C}_3\text{SO}_3\text{HPy}]\text{H}_2\text{PO}_4$ , which is consistent with the activity order of the SFILs to hydrolyse chitosan. Furthermore, the effect of reaction time was examined. With  $[\text{C}_3\text{SO}_3\text{HPy}]\text{HSO}_4$  as catalyst, the viscosity-average molecular weight ( $M_v$ ) of chitosan dropped continuously from the beginning 560 000 to 24 167 (30 s), 882 (90 s), and 450 (120 s). Meanwhile, the TRS yield increased from 15% (30 s) to 84% (90 s) and 92% (120 s). They attributed the high yield of TRS to the combination of ILs, SFILs and MW. Wu *et al.*'s homogeneous depolymerization of chitosan to TRS<sup>56</sup> suggested a depolymerization mechanism: first, complete dissolution of chitosan in mixed ILs enables 1,4- $\beta$ -glycosidic bonds to be more accessible to the catalytic species  $\text{H}^+$ . Secondly, ILs with high polarity absorb MW emission and markedly accelerate the reaction rate compared to conventional heating in an oil bath.

## 2.3 HMF

Owing to the bifunctional aldehyde and hydroxyl groups, HMF has been selected by the US Department of Energy as one of the top 12 platform chemicals from biomass for the production of various valuable chemicals, *e.g.*, 2,5-furandicarboxylic acid (monomer of terephthalate alternatives),<sup>72,73</sup> 2,5-dimethylfuran (fuel),<sup>74,75</sup> furan-2,5-dicarbaldehyde (chemical intermediate),<sup>76,77</sup> and levulinic acid (platform chemical).<sup>78</sup> In comparison with a large number of research on HMF preparation from lignocellulosic biomass,<sup>5,44,46,79–81</sup> there are only a few reports on the conversion of chitosan to HMF. Kerton and co-workers<sup>71</sup> hydrolyzed chitosan to HMF in 10.0% yield with  $\text{SnCl}_4 \cdot 5\text{H}_2\text{O}$  as a catalyst under MW irradiation, whereas they found higher yield of HMF was obtained under dilute conditions *versus* more concentrated conditions. The proposed mechanism of HMF formation from chitosan monomer by deamination is shown in Fig. 3. Meanwhile, Qiao and Hou<sup>25</sup> obtained HMF (12.8%) from chitosan using concentrated  $\text{ZnCl}_2$  aqueous solution. Lee *et al.*<sup>82</sup> used  $\text{H}_2\text{SO}_4$  to hydrolyze chitosan to HMF in 12.1% yield at 174 °C.

Zang and co-workers<sup>57</sup> screened nine ILs to catalyze chitosan conversion into HMF, including  $[\text{C}_4\text{mim}]\text{HSO}_4$ ,  $[\text{C}_4\text{mim}]\text{BF}_4$ ,  $[\text{C}_4\text{mim}]\text{Cl}$ ,  $[\text{C}_4\text{mim}]\text{Br}$ ,  $[(\text{C}_4\text{SO}_3\text{H})_2\text{im}]\text{HSO}_4$ ,  $[\text{Hmim}]\text{HSO}_4$ ,  $[\text{Hmim}]\text{Cl}$ ,  $[\text{C}_4\text{SO}_3\text{Hmim}]\text{HSO}_4$ , and  $[\text{CH}_2\text{COOHmim}]\text{Cl}$  (Table 1, entry 3). The effect of IL structure on the yield of HMF was investigated. The acidic ILs  $[(\text{C}_4\text{SO}_3\text{H})_2\text{im}]\text{HSO}_4$ ,  $[\text{Hmim}]\text{HSO}_4$ ,  $[\text{C}_4\text{SO}_3\text{Hmim}]\text{HSO}_4$ ,  $[\text{CH}_2\text{COOHmim}]\text{Cl}$  showed stronger catalytic activity than some neutral ILs  $[(\text{C}_4\text{mim})\text{Cl}]$ ,  $[\text{C}_4\text{mim}]\text{Br}$ , which failed to catalyze chitosan conversion. It was proposed that the intramolecular H-bonds of chitosan from  $-\text{OH}$  and  $-\text{NH}_2$  groups were broken by the interaction with  $\text{H}^+$  leading to new intermolecular H-bonds, so that the breakage of glycosidic bonds was accelerated and chitosan hydrolysis was promoted. With the same cationic structure, ILs with acidic anions  $[(\text{C}_4\text{mim})\text{HSO}_4]$ ,  $[\text{Hmim}]\text{HSO}_4$  showed stronger catalytic activity than those with neutral anions  $[(\text{C}_4\text{mim})\text{BF}_4]$ ,  $[\text{C}_4\text{mim}]\text{Cl}$ ,  $[\text{C}_4\text{mim}]\text{Br}$ ,  $[\text{Hmim}]\text{Cl}$ . When  $\text{Cl}^-$  was fixed as the anion, the IL with an acidic cation  $[(\text{CH}_2\text{COOHmim})\text{Cl}]$  showed stronger catalytic



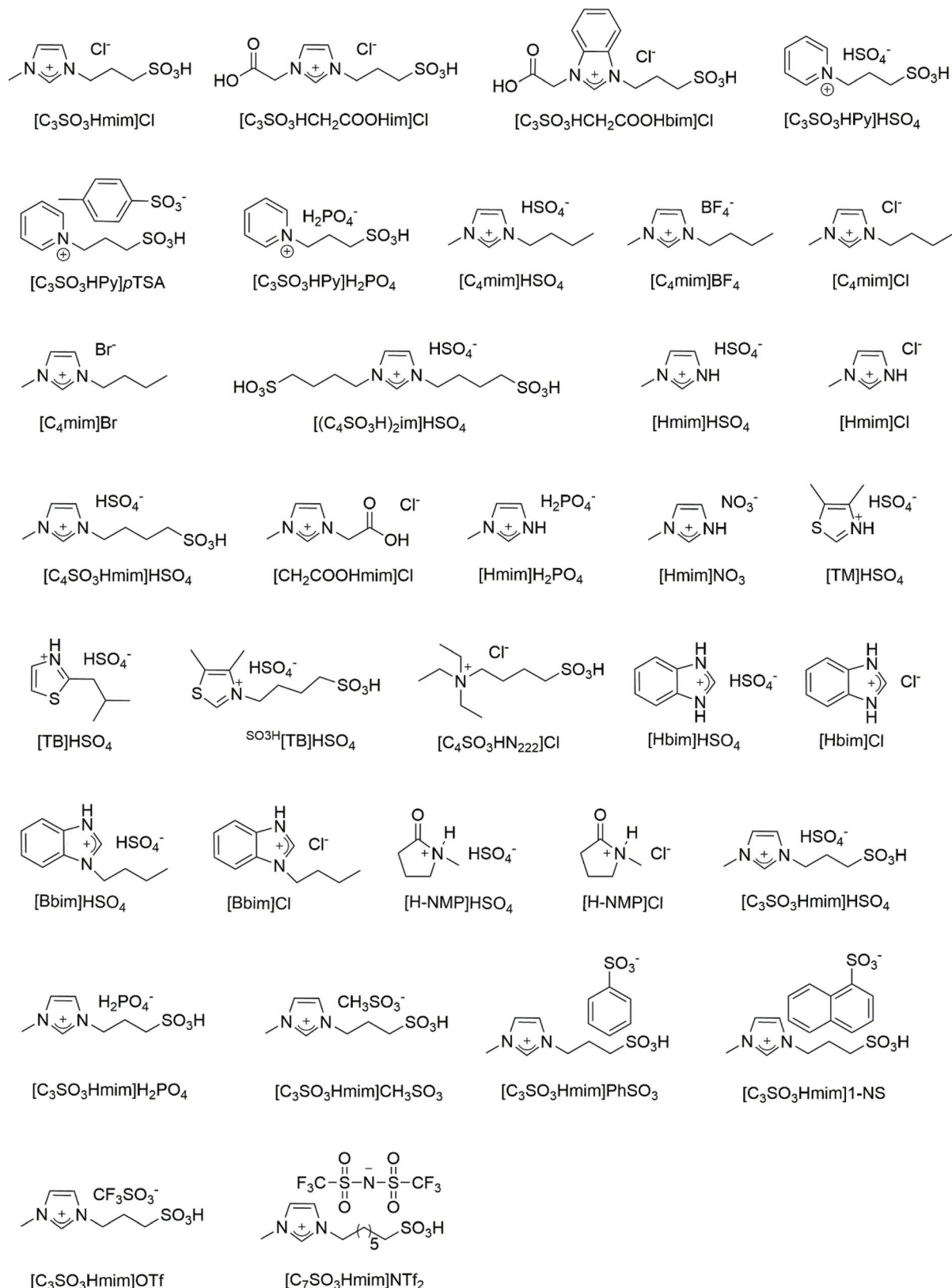


Fig. 2 The structure of acidic ILs referred to in this review by the order of appearance.

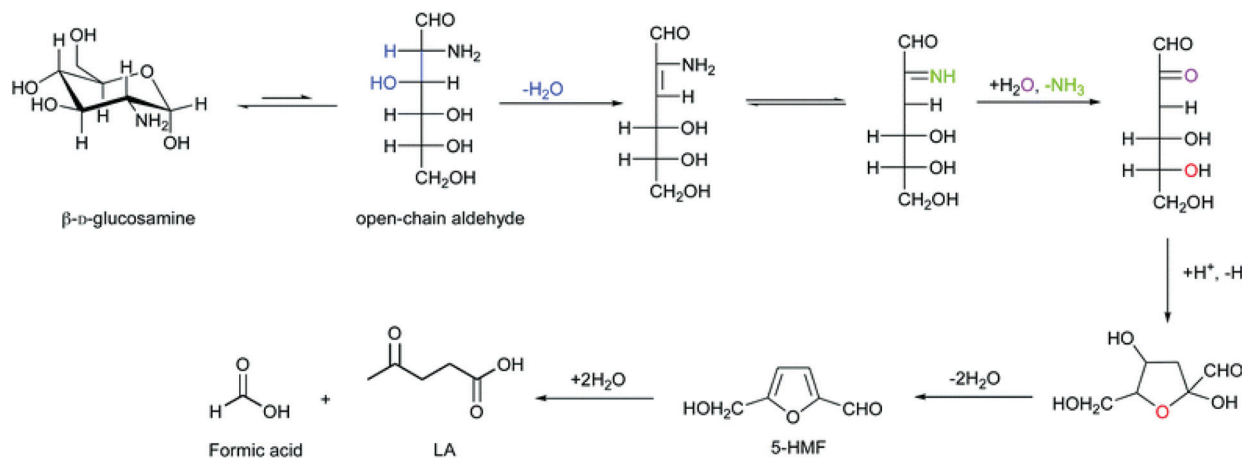


Fig. 3 Proposed mechanism for HMF and LA from chitosan monomer. Figure reproduced from ref. 71 with kind permission from The Royal Society of Chemistry.

activity than those with neutral cations ( $[\text{C}_4\text{mim}]\text{Cl}$ ,  $[\text{Hmim}]\text{Cl}$ ). When  $\text{HSO}_4^-$  was used as the anion, likewise, ILs with more acidic cations should show stronger catalytic activity. However,  $[(\text{C}_4\text{SO}_3\text{H})_2\text{im}]\text{HSO}_4$  and  $[\text{C}_4\text{SO}_3\text{Hmim}]\text{HSO}_4$ , which are more acidic, showed lower catalytic activity than  $[\text{C}_4\text{mim}]\text{HSO}_4$  and  $[\text{Hmim}]\text{HSO}_4$ . This could be ascribed to the steric hindrance of the longer  $\text{SO}_3\text{H}$  group, thus enabling the ILs difficult to enter chitosan and decreasing the catalytic activity accordingly. Hence, it was suggested that the acidity and structure of ILs play key roles in the catalysis of chitosan conversion. Among the ILs,  $[\text{Hmim}]\text{HSO}_4$  led to the highest HMF yield of 21.7 mol%, due to the dual effects of the cationic and anionic structures. As the amount of IL increased from 2 wt% to 4 wt%, the yield of HMF reached a maximum of 29.5 mol% at 180 °C for 5 h (Table 1, entry 3). Another possible mechanism of deamination proposed is shown in Fig. 4, wherein an open-chain form was initially formed, followed by isomerization to the enol-intermediate and then the formation of a five-membered ring with the  $-\text{NH}_2$  group removed from GlcN. It was assumed that the so-formed five-membered compounds are key intermediates towards the formation of HMF.

When the  $\text{DMSO}/\text{H}_2\text{O}$  mixture solvent was used instead of a single water solvent,<sup>58,83</sup> the conversion yield of chitosan to HMF could be improved to 34.7% with  $[\text{Hmim}]\text{HSO}_4$  as a catalyst at 180 °C for 6 h, probably due to the suppression of humin byproducts (Table 1, entry 4).

Furthermore, by combining the advantages of a Brønsted acid and a Lewis acid, the mixed-type Brønsted–Lewis acidic IL catalysts<sup>59</sup> were employed in the conversion of chitosan, and the HMF yield was further improved to 44.1% by catalysis of  $[\text{Hmim}]\text{HSO}_4$ –0.5 $\text{FeCl}_2$  at 180 °C for 4 h (Table 1, entry 5).

In addition to  $[\text{Hmim}]\text{HSO}_4$ , benzimidazole-based ILs that can be synthesized from environmentally friendly and biocompatible benzimidazole, were used to catalyze the conversion of chitosan at 180 °C for 3 h, leading to a higher HMF yield of 34.9% in the  $\text{DMSO}/\text{H}_2\text{O}$  mixed solvent than 30.8% in pure water for  $[\text{Hbim}]\text{Cl}$ .<sup>60</sup> In comparison,  $[\text{Bbim}]$ -type ILs were less

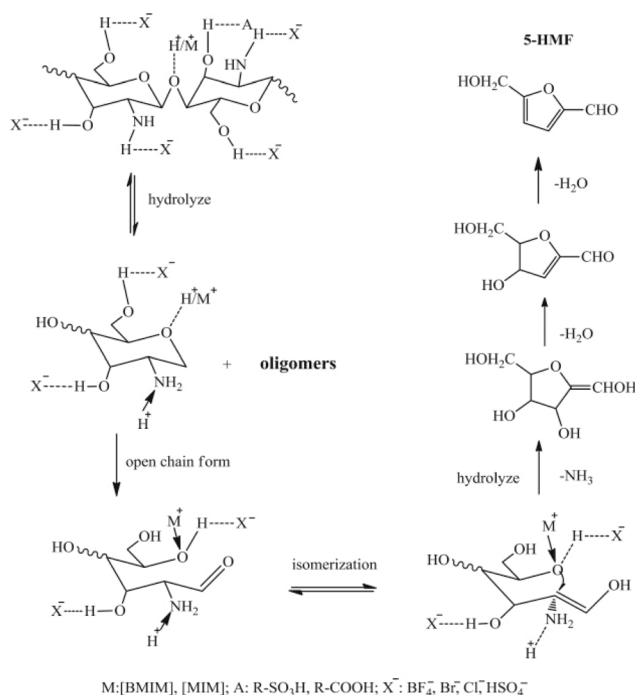


Fig. 4 Proposed mechanism of chitosan conversion to HMF. Figure reproduced from ref. 57 with kind permission from Elsevier.

effective probably due to the increased steric hindrance after substitution of H at the 1-position by a butyl group (Table 1, entry 6).

## 2.4 LA

Due to the bifunctional carboxylic and keto groups, levulinic acid (LA) has also been widely recognized as one of the top 12 platform chemicals to produce a variety of downstream chemicals, for example, 5-bromolevulinic acid (pharmaceutical agent), ethyl levulinate (flavor compound), 5-nonanone (fuel),

$\delta$ -aminolevulinic acid (herbicide),  $\gamma$ -valerolactone (solvent), succinic acid (plasticiser), and nylon-6,6 (polymer).<sup>84–90</sup> Biomass conversion to produce LA was reported to be able to bridge with petroleum processing, thus becoming critical in biorefining.<sup>15,67,68,71,78,91–97</sup> Chitosan conversion to LA has recently attracted increasing attention. Kerton and co-workers<sup>71</sup> hydrolysed chitosan by the catalysis of  $\text{SnCl}_4 \cdot 5\text{H}_2\text{O}$  under MW irradiation at 200 °C for 30 min, leading to a LA yield of 23.9 wt% (33.2 mol%). Mika and co-workers<sup>97</sup> degraded chitosan in the presence of  $\text{H}_2\text{SO}_4$  and HCl catalysts under MW irradiation at 190 °C for 20 min, resulting in a LA yield of 19.3–37.0 mol%. To date, efficiently converting chitosan into LA still remains challenging.

Based on our previous research on the production of LA by IL-catalysed conversion of cellulose<sup>45,67</sup> and lignocellulose,<sup>68</sup> we further expanded to convert chitosan to LA.<sup>61</sup> By the catalysis of  $[\text{C}_3\text{SO}_3\text{Hmim}]\text{HSO}_4$  at 170 °C for 5 h, the yield of LA was significantly increased to 64% at a lower chitosan intake of 50 mg. It was inferred that lower reactive intermediate concentration could inhibit the intermolecular polymerization to humin byproducts,<sup>98–105</sup> thus promoting the intramolecular conversion of chitosan to the LA target product (Table 1, entry 7).

The relationship between acidic IL structure and the yield of LA was studied next. The Brønsted acidity of six acidic ILs was determined by the Hammett method.<sup>67</sup> For  $[\text{C}_3\text{SO}_3\text{Hmim}]$ -type ILs, the acidities of the ILs decreased in the sequence  $\text{HSO}_4^- > \text{PhSO}_3^- \sim \text{CH}_3\text{SO}_3^- > \text{Cl}^- > 1\text{-NS} > \text{H}_2\text{PO}_4^-$ . Consequently, a stronger acidity of IL led to a higher LA yield obtained from chitosan, thus suggesting the critical role of acidity for IL catalysts during chitosan conversion, presumably through protonation of the glycosidic bond.

Noticeably, for cellulose feedstock,  $[\text{C}_3\text{SO}_3\text{Hmim}]\text{Cl}$  led to higher LA yield than  $[\text{C}_3\text{SO}_3\text{Hmim}]\text{HSO}_4$ , although  $[\text{C}_3\text{SO}_3\text{Hmim}]\text{Cl}$  is less acidic than  $[\text{C}_3\text{SO}_3\text{Hmim}]\text{HSO}_4$ .<sup>67</sup> This could be ascribed to the stronger H-bonding acceptors of  $\text{Cl}^-$  that break the H-bonding network in cellulose,<sup>38,106–108</sup> thus enhancing the accessibility of the IL catalyst to the catalytic sites in cellulose and improving the catalytic activity of IL.

In comparison, for chitosan feedstock, the H-bonding ability of IL had no prominent effect on chitosan conversion as in the case of cellulose. Even though due to the stronger H-bonding ability of  $\text{Cl}^-$ , the solubility of chitosan could indeed be improved from 0% ( $[\text{C}_3\text{SO}_3\text{Hmim}]\text{HSO}_4$ ) to ca. 5% ( $[\text{C}_3\text{SO}_3\text{Hmim}]\text{Cl}$ ) in the presence of water (3.31 mmol of IL and 4.000 g of water), the yield of LA catalyzed by  $[\text{C}_3\text{SO}_3\text{Hmim}]\text{Cl}$  was still lower than that by  $[\text{C}_3\text{SO}_3\text{Hmim}]\text{HSO}_4$ . This could be explained that the quaternization interactions between the  $-\text{NH}_2$  groups of chitosan and acidic IL dominate over the H-bonding interactions. As a result, the yield of LA from chitosan conversion was solely dictated by the acidity of IL, rather than the H-bonding ability of IL. It can be seen that the IL structure has different effects on the yield of LA due to the presence of  $-\text{NH}_2$  group in chitosan feedstock *versus* cellulose feedstock.

### 3. Conversion of chitin to chemicals catalysed by ILs

The acetamide groups account for the huge differences between chitin and cellulose, which contribute to an even stronger H-bonding network in chitin compared to chitosan.<sup>109</sup> The earlier applications of ILs in chitin research were mostly concentrated on chitin dissolution,<sup>49–52,54,107,110–112</sup> which has been thoroughly reviewed recently. Dissolution of chitin in ILs is based on the principle that ILs could form new hydrogen bonds with chitin to disrupt the original inter- and intramolecular H-bonds in the chitin polymer.<sup>52</sup> Zhao and co-workers converted chitin to TRS at 25% using HCl as the catalyst and  $[\text{C}_4\text{mim}]\text{Cl}$  as the solvent.<sup>54</sup> Reports of ILs as catalysts for chitin conversion have been rather limited. One example is that of  $[\text{Hmim}]\text{HSO}_4$  adopted to convert chitin into HMF at 19.3%.<sup>57</sup> Recently, we explored the selective conversion of chitin to LA (67.0%) catalysed by acidic IL,<sup>113</sup> in comparison with our aforementioned research on IL-catalysed conversion of chitosan,<sup>61</sup> demonstrating the effect of the acetamido group on chitin conversion.

#### 3.1 TRS

Zhao and co-workers<sup>54</sup> hydrolysed chitin using HCl as the catalyst and  $[\text{C}_4\text{mim}]\text{Cl}$  as the solvent at 100 °C for 7 h, leading to a yield of 25% for TRS, which was much lower than that of chitosan (63%). They noticed the increased viscosity of the reaction mixture for chitin and suggested that other complex products were formed under these conditions. In comparison with chitosan, more efforts are needed for chitin feedstock to achieve efficient hydrolysis.

Reichert and Davis<sup>62</sup> also chose  $[\text{C}_4\text{mim}]\text{Cl}$  to prepare a 1 wt% chitin solution, whereas the IL with  $\text{OAc}^-$  was found to deactivate the catalyst causing chitin unable to hydrolyze. Afterwards, alkyl chain SFILs were used to catalyze chitin hydrolysis. With  $[\text{C}_3\text{SO}_3\text{Hmim}]\text{OTf}$  as the catalyst, the yield of *N*-acetyl-D-glucosamine (GlcNAc) increased from 6% to 15% as the reaction temperature increased from 100 °C to 120 °C. Changing the catalyst to  $[\text{C}_7\text{SO}_3\text{Hmim}]\text{NTf}_2$  made the product GlcNAc undetectable, probably due to the degradation of GlcNAc (Table 1, entry 8).

#### 3.2 3A5AF

Chitin is made up of GlcNAc monomers, which are nitrogenous monosaccharides. The unique structure of chitin holds great potential in the production of nitrogen-containing compounds that cannot be obtained from lignocellulosic biomass.

Kerton and co-workers<sup>71</sup> initially obtained LA from chitosan and GlcN in water medium. Nevertheless, when the transformation of GlcNAc was conducted in dipolar aprotic solvents or imidazolium ILs in the presence of  $\text{Cl}^-$  and boric acid, 3A5AF was obtained.<sup>24,114</sup> Under both circumstances, 60% yield of 3A5AF could be achieved, which was 30 times higher than the pyrolysis route. Later, Kerton and Yan<sup>115</sup> reported that chitin could be directly converted into 7.5% yield of 3A5AF in

*N*-methyl-2-pyrrolidone (NMP) solvent with alkaline chlorides and boric acid as additives at 215 °C for 1 h.

Furthermore, Kerton and Yan<sup>116</sup> tested 10 ILs as the solvent and screened 25 additives, suggesting that solubility was not the crucial factor and Cl<sup>−</sup> may participate in the reaction since 3A5AF could not be produced without Cl<sup>−</sup>. The yield of 3A5AF was improved from less than 1% to 6.2% in [C<sub>4</sub>mim]Cl with HCl and boric acid as additives at 180 °C for 1 h, whereas the reaction temperature was lower than in organic solvents (215 °C). The enhanced yield was ascribed to the synergistic effects of the two additives, whereas the acids catalyzed chitin hydrolysis to the monomers and boric acid promoted the subsequent dehydration step. In addition, the concept whether acidic ILs could replace the neutral ILs with acidic additives was tested on GlcNAc. It was found that the addition of 1 and 2 equivalents of NaCl to the reaction in [C<sub>4</sub>mim]HSO<sub>4</sub> could increase the 3A5AF yield from 10.7% (in the absence of NaCl) to 15.4% and 19.7%, respectively. These results confirmed the crucial role of Cl<sup>−</sup> in chitin conversion towards 3A5AF, indicating that acidic ILs were less effective for the production of 3A5AF.

### 3.3 HMF

Kerton and co-workers<sup>71</sup> hydrolyzed chitin using SnCl<sub>4</sub>·5H<sub>2</sub>O as the catalyst under MW irradiation and no HMF was produced with only LA detected. In comparison, Qiao and Hou<sup>25</sup> obtained HMF in 9.0% yield from chitin using concentrated ZnCl<sub>2</sub> aqueous solution. Zang and co-workers<sup>57</sup> hydrolyzed chitin in [Hmim]HSO<sub>4</sub> at 180 °C for 5 h, leading to a higher HMF yield of 19.3% (Table 1, entry 9). When DMSO/H<sub>2</sub>O mixture solvent was used instead of a single water solvent,<sup>58</sup> the conversion yield of chitin to HMF could be improved to 25.7% with [Hmim]HSO<sub>4</sub> as the catalyst, probably due to the suppression of humin by-product (Table 1, entry 10).

### 3.4 LA

Kerton and co-workers<sup>71</sup> hydrolyzed chitin to LA in 12.7% yield using SnCl<sub>4</sub>·5H<sub>2</sub>O as the catalyst under MW irradiation. Due to the stronger hydrogen bonding network in chitin, highly efficient conversion of chitin is more difficult.

On the basis of our research on selective chitosan conversion to LA, we proceeded to investigate the conversion of chitin into LA by the catalysis of ILs, whereas 67.0% yield of LA was achieved at a lower feedstock intake with [C<sub>3</sub>SO<sub>3</sub>Hmim]HSO<sub>4</sub> as the catalyst at 180 °C for 5 h (Table 1, entry 11).<sup>63</sup> The effect of IL structure on conversion efficiency of chitin was also examined. The Brønsted acidity of six acidic ILs was quantified and followed the sequence HSO<sub>4</sub><sup>−</sup> > PhSO<sub>3</sub><sup>−</sup> ~ CH<sub>3</sub>SO<sub>3</sub><sup>−</sup> > Cl<sup>−</sup> > 1-NS > H<sub>2</sub>PO<sub>4</sub><sup>−</sup>. According to the catalytic outcome, the IL with stronger acidity led to a higher LA yield, thus demonstrating the crucial role of acidity during the catalytic conversion of chitin.

One exception is [C<sub>3</sub>SO<sub>3</sub>Hmim]Cl resulting in 54.0% yield of LA, which is particularly high but does not overtake [C<sub>3</sub>SO<sub>3</sub>Hmim]HSO<sub>4</sub> (56.5%). As learnt from our previous research,<sup>67</sup> [C<sub>3</sub>SO<sub>3</sub>Hmim]Cl could result in a higher yield of LA

as compared to [C<sub>3</sub>SO<sub>3</sub>Hmim]HSO<sub>4</sub> for cellulose feedstock. Therefore, it was proposed that the LA yield in the presence of 3.31 mmol of [C<sub>3</sub>SO<sub>3</sub>Hmim]Cl might not reach the maximum yield for chitin feedstock, since deamination causes a decrease of IL acidity. When the dosage of [C<sub>3</sub>SO<sub>3</sub>Hmim]Cl was increased to 4.97 mmol, the LA yield from chitin conversion indeed improved to 61.5% and levelled off, which verified our hypothesis. Hence, after ruling out the factor of acidity loss, the strong H-bonding ability of Cl<sup>−</sup> predominated and surpassed [C<sub>3</sub>SO<sub>3</sub>Hmim]HSO<sub>4</sub>, although the acidity of [C<sub>3</sub>SO<sub>3</sub>Hmim]Cl is lower than that of [C<sub>3</sub>SO<sub>3</sub>Hmim]HSO<sub>4</sub>. It can be seen that the effect of IL structure on the LA yield for chitin feedstock not only resembles that for cellulose feedstock wherein the stronger H-bonding acceptor of Cl<sup>−</sup> helps to break the original H-bonding network<sup>38,106</sup> and enhances the accessibility of the IL catalyst to the catalytic sites, but also resembles that for chitosan feedstock wherein deamination occurs causing acidity loss.

## 4. Conversion of crustacean shells to chemicals catalysed by ILs

The main components in raw crustacean shells are chitin, protein, and calcium carbonate. Chitin functions as the skeleton, with calcium carbonate imparting the necessary strength and proteins endowing a living tissue.<sup>117</sup> The traditional process to separate the chitin component from crustacean shells includes demineralization by acidic treatment and then deproteinization by alkaline treatment.<sup>118,119</sup> Lately, in order to upgrade to green technologies, ILs have been employed in chitin production.<sup>52,120,121</sup>

Rogers' group first adopted [C<sub>2</sub>mim]OAc to extract chitin from shrimp shells,<sup>51</sup> from which the resultant chitin solution in [C<sub>2</sub>mim]OAc can be further used to fabricate nanomats,<sup>122</sup> fibers,<sup>123</sup> hydrogels,<sup>124</sup> and films.<sup>125</sup> Through comparison, only chitin which is extracted by IL can produce strong films,<sup>125</sup> while the commercially available chitin cannot. In addition, ILs can be designed toward deproteinization, whereas chitin separation could be realized alternatively not through chitin extraction. Rogers' group used [NH<sub>3</sub>OH][OAc] to deproteinize and demineralize from shrimp shells, leading to chitin separation with over 80% purity.<sup>126</sup> Zhang and co-workers adopted phosphate IL [C<sub>2</sub>mim]DMP for deproteinization, followed by Zn(OAc)<sub>2</sub> for demineralization, offering a green method to produce chitin/Zn composite directly from shrimp shells.<sup>127</sup>

Compared with chitin separation from crustacean shells, the conversion of crustacean shells to chemicals has just started. Yan and Jin converted shrimp shells by oxidation of CuO and O<sub>2</sub> in 2 M NaOH solution, leading to HOAc at a yield of 47.9%.<sup>26</sup> Yan's group transformed shrimp shells into low *M<sub>w</sub>* chitosan by NaOH catalysed mechanochemistry.<sup>32</sup> Recently, they came up with an integrated process whereas the shell waste was converted into tyrosine and L-DOPA by a microbial engineering method after pretreatment.<sup>128</sup> The econ-



omic advantage will be greatly enhanced if the raw crustacean shells could be efficiently converted to high value-added chemicals, thus combining chitin separation and conversion of chitin into one step. Application of ILs as the catalyst to convert raw crustacean shells has not yet been reported. Following our systematic research on IL-catalysed conversion of chitosan<sup>61</sup> and chitin,<sup>63</sup> we continued to investigate the conversion of raw crustacean shells into LA by the catalysis of acidic ILs, unveiling the difference between chitin and crustacean shells.<sup>64</sup>

#### 4.1 LA

For 250 mg of crab shells, 1.5 g of  $[\text{C}_3\text{SO}_3\text{Hmim}]\text{HSO}_4$  was required to reach the maximum yield of LA, but only 1.0 g of  $[\text{C}_3\text{SO}_3\text{Hmim}]\text{HSO}_4$  was needed for 250 mg of chitin feedstock. This could be ascribed to higher acid consumption by both deamination and the  $\text{CaCO}_3$  component. By catalysis of  $[\text{C}_3\text{SO}_3\text{Hmim}]\text{HSO}_4$ , the yield of LA could be improved to 77.9% at a lower intake of crab shells at 180 °C for 5 h (Table 1, entry 12).<sup>64</sup>

The relationship between the structure of ILs and conversion efficiency of crab shells was investigated next. The Hammett acidity function ( $H_0$ ) of six acidic ILs was measured to evaluate the Brønsted acidity, and the acidities follow the sequence  $\text{HSO}_4^- > \text{PhSO}_3^- \sim \text{CH}_3\text{SO}_3^- > \text{Cl}^- > 1\text{-NS} > \text{H}_2\text{PO}_4^-$ . The yields of LA from the conversion of crab shells mostly agree with the acidity sequence of ILs, highlighting the essential role of acidity for IL catalysts.

The only exception is  $[\text{C}_3\text{SO}_3\text{Hmim}]\text{Cl}$ , whose acidity is lower than  $[\text{C}_3\text{SO}_3\text{Hmim}]\text{HSO}_4$  but leads to higher LA yield (77.6%) surpassing  $[\text{C}_3\text{SO}_3\text{Hmim}]\text{HSO}_4$  (62.6%). It can be seen that the effect of IL structure on the LA yield for crab shells resembles that for cellulose feedstock. During the conversion of crab shells, the  $\text{Cl}^-$  anion can destroy the original H-bonding network to form new strong hydrogen bonds with the chitin fraction<sup>38,106</sup> in the crab shells, thus enabling chitin greater access to the cationic structure of the IL through the ion–dipole interactions between the anions and cations of the IL. Therefore, it becomes easier for the  $\text{SO}_3\text{H}$  groups on the cation to protonate the  $\beta$ -glycosidic linkages within the chitin fraction and promote the hydrolysis reaction to produce LA. By the analogy with an enzyme comprising binding domain and catalytic domain,<sup>46</sup> the mechanism underlying how IL catalysts work could be understood intuitively, whereas  $\text{Cl}^-$  and  $\text{SO}_3\text{H}$  groups function as the binding domain and the catalytic domain, respectively. Hence, the stronger H-bonding ability of  $\text{Cl}^-$  helps to improve access of the  $\text{SO}_3\text{H}$  group to the chitin component and enhances the catalytic efficiency of IL towards the LA product.

The reason that the effect of the IL structure on the LA yield for crab shells does not resemble that for chitin feedstock was attributed to the use of 1.5 g of IL, which makes up for the acidity loss caused by deamination and the  $\text{CaCO}_3$  component in crab shells. Thus, the effect of the IL structure on the yield of LA for crustacean shells has been unraveled, which is different from chitin feedstock. Furthermore, the self-healing

phenomenon of the chitin fraction in crab shells was discovered after the removal of  $\text{CaCO}_3$  and protein as driven by the strong hydrogen bonds (Fig. 5).

## 5. Separation of products and recyclability of ILs

For practical applications of industrial processes, it is necessary to separate the products and recycle the ILs efficiently. So far, a big portion of the research work on conversion of marine biomass is still at the preliminary stage of methodology development. Only a few have managed to realize the separation of the products and reuse of the ILs.

### 5.1 Separation of products

For production of chitosan oligomers from chitosan conversion, Dandekar *et al.*<sup>55</sup> used acetone as the anti-solvent to precipitate chitosan oligomers from the IL reaction mixture and the chitosan oligomers could be separated by cold centrifugation. Alternatively,  $\text{Na}_2\text{CO}_3$  was added to precipitate the chitosan oligomers which could be separated after centrifugation and washing till neutral.

For HMF product, some organic solvents (*e.g.* tetrahydrofuran, toluene, ether, ethyl acetate) were traditionally employed to separate HMF by extraction.<sup>129–131</sup> Recently, efficient extraction of HMF from glucose conversion in  $[\text{C}_4\text{mim}]\text{Cl}$  has been reported by charging compressed  $\text{CO}_2$  into the reaction mixtures.<sup>132</sup> Zang *et al.* found ethyl acetate was the best solvent to extract HMF from chitosan conversion by catalysis of  $[\text{Hmim}][\text{HSO}_4]$ ,  $[\text{Hmim}]\text{HSO}_4\text{--}0.5\text{FeCl}_2$  or  $[\text{Hbim}]\text{Cl}$ .<sup>57–60</sup>

For LA product, as early as 2013, we have demonstrated good recyclability of the acidic IL  $[\text{C}_3\text{SO}_3\text{Hmim}]\text{HSO}_4$  for the conversion of cellulose feedstock, after esterification of the LA product followed by a facile phase separation.<sup>45</sup> Two years later, we found out that the LA product can be directly separated by methyl isobutyl ketone (MIBK) extraction, and the efficiency of extracting LA can reach 98%.<sup>67,133</sup> Meanwhile, the LA product can be simply purified from MIBK by distillation and MIBK is also reusable. Afterwards, we found that the separation of LA product by MIBK extraction could be applied for feedstocks of chitosan,<sup>61</sup> chitin<sup>63</sup> and crustacean shells.<sup>64</sup>

### 5.2 Recyclability of ILs

As discussed above, one of the advantages of IL is their structural designability, whereas the desired performance can be achieved by modulating cationic and anionic structures of ILs. Beyond that, another advantage of ILs is their recyclability,<sup>35–37</sup> which will be discussed taking LA as an example. For cellulose feedstock, the recycling performance of ILs was measured after phase separation from MIBK extractant followed by vacuum drying. The LA yield did not decrease, but rose slightly from 58.5% to 65.7% after five cycles (Fig. 6), showing that the acidic IL maintained stable catalytic activity. The slight increase in LA yield was ascribed to the residual oligomers that can transform into LA in the next cycle.

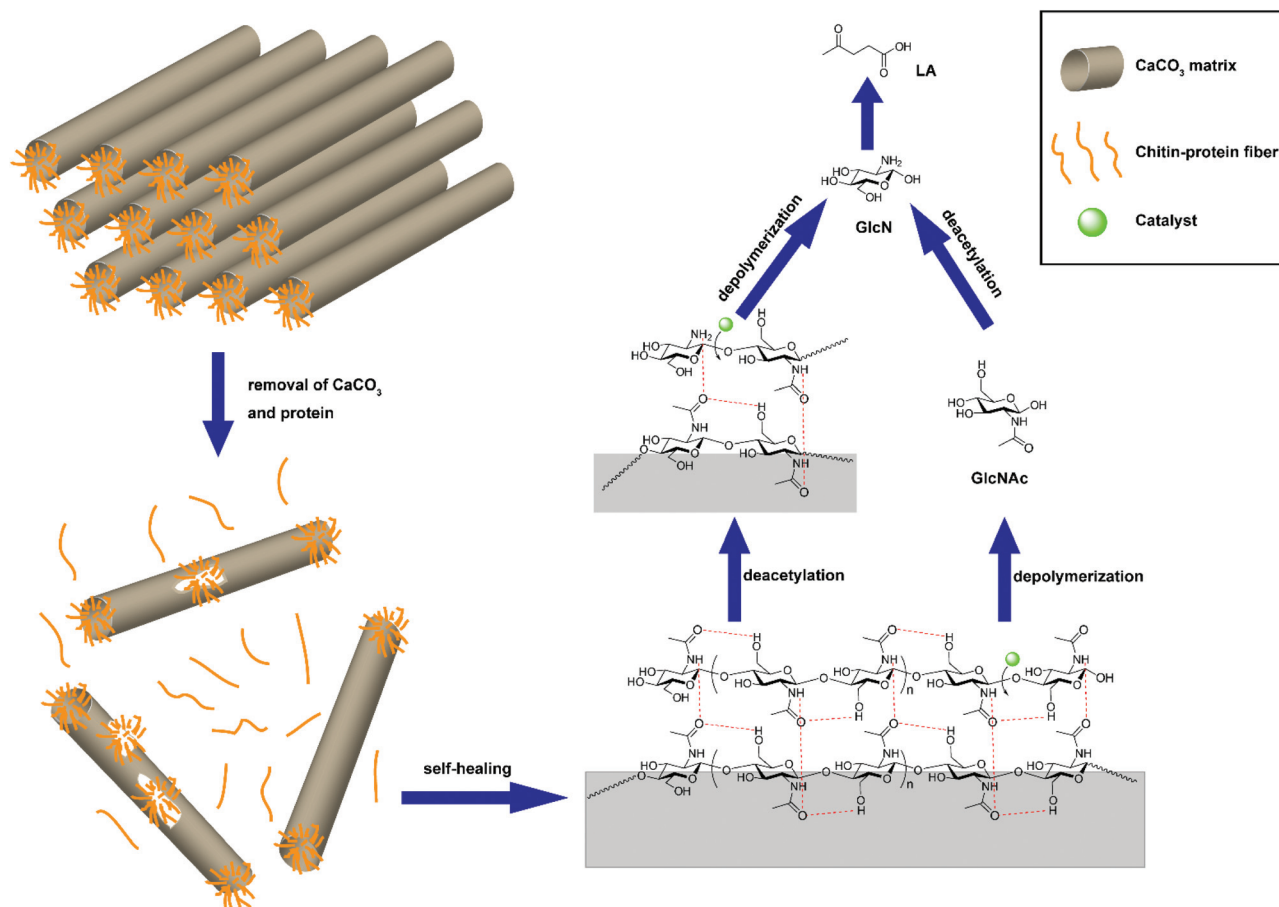


Fig. 5 Self-healing of chitin fraction during conversion of crab shells. Figure reproduced from ref. 64 with kind permission from the American Chemical Society.

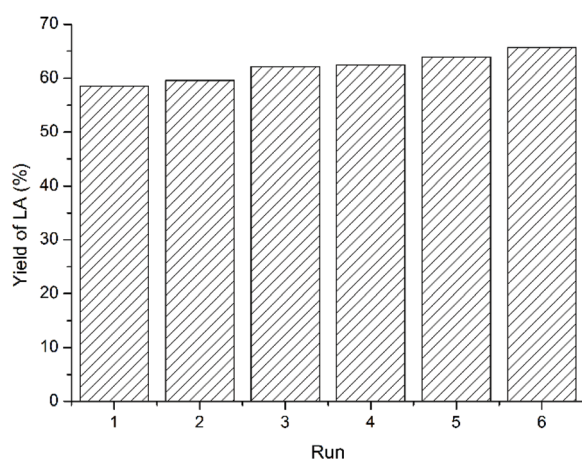


Fig. 6 The reuse of IL for cellulose feedstock. Figure reproduced from ref. 67 with kind permission from Elsevier.

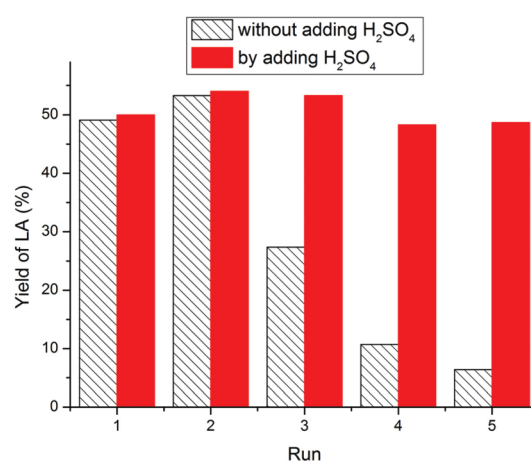


Fig. 7 The reuse of IL for chitosan feedstock. Figure reproduced from ref. 61 with kind permission from Elsevier.

In comparison with cellulose feedstock, the IL recyclability of acidic IL differs significantly for marine biomass including chitosan, chitin, and crustacean shells, which will be discussed in turn according to the aforementioned order of feedstock from simple to complex.

For chitosan feedstock (Fig. 7), the LA yield increased slightly from 49.1% (first cycle) to 53.3% (second cycle), since the residual oligomers could transform to LA in the latter cycle. Surprisingly, during the following cycles, the LA yield

declined to 27.4%, 10.7% and 6.4%, respectively. It was assumed that the catalytic activity was reduced due to deamination that led to a decrease in IL acidity. To prove this hypothesis, 1 equivalent of  $\text{H}_2\text{SO}_4$  was supplemented to the recovered IL to make up for the acidity loss. Thereafter, the recovered IL could be recycled over five times without appreciable decrease in LA yield.<sup>61</sup>

Though deamination from chitosan has been proposed previously,<sup>26,66,71,97</sup> efforts to detect  $\text{NH}_3$  have been unsuccessful. In 2018, the typical triplet peaks were accidentally observed on the  $^1\text{H}$  NMR spectra of the reaction mixture and they could be assigned to  $\text{NH}_4^+$  by comparison with standard  $\text{NH}_4\text{HSO}_4$  (Fig. 8). In addition, 15.3 mg of  $\text{NH}_4^+$  was quantified by ion chromatography, indicating that 54.6% of the  $-\text{NH}_2$  group on chitosan has been converted to  $\text{NH}_4^+$ . It is reasonably higher than LA yield (49.0%) because  $\text{NH}_3$  elimination occurs prior to LA formation. To the best of our knowledge, this is the first report of clear evidence for deamination during chitosan conversion.<sup>61</sup>

For chitin feedstock (Fig. 9), the yield of LA decreased from 56.5% (first cycle) to 48.5% (second cycle), 46.0% (third cycle), 40.4% (fourth cycle), and 34.9% (fifth cycle). The reduced catalytic activity could be also attributed to  $\text{NH}_3$  elimination during conversion of chitin resulting in a decrease in IL acidity. On analysis of the reaction mixture, characteristic triplet peaks corresponding to  $\text{NH}_4^+$  appeared on the  $^1\text{H}$  NMR spectra confirming deamination during chitin conversion.<sup>26,71,83,97</sup> Moreover, to compensate for the acidity loss, 1 equivalent of  $\text{H}_2\text{SO}_4$  was added to the reused IL and the LA yield did not decrease noticeably over five times.<sup>63</sup>

For the raw crab shells (Fig. 10), the yield of LA dropped down from 62.8% (first cycle) to 54.0% (second cycle), 22.1% (third cycle), 0% (fourth cycle), and 0% (fifth cycle). This dra-

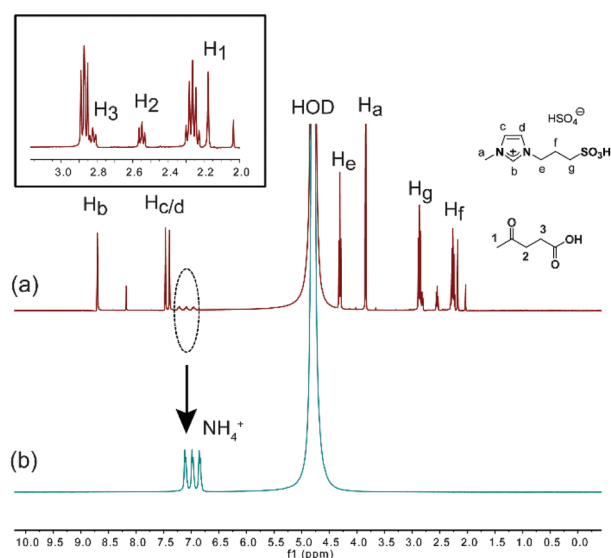


Fig. 8  $^1\text{H}$  NMR spectra (in  $\text{D}_2\text{O}$ ) of (a) reaction mixture of chitosan by  $[\text{C}_3\text{SO}_3\text{Hmim}]\text{HSO}_4$  catalysis and (b) standard  $\text{NH}_4\text{HSO}_4$ . Figure reproduced from ref. 61 with kind permission from Elsevier.

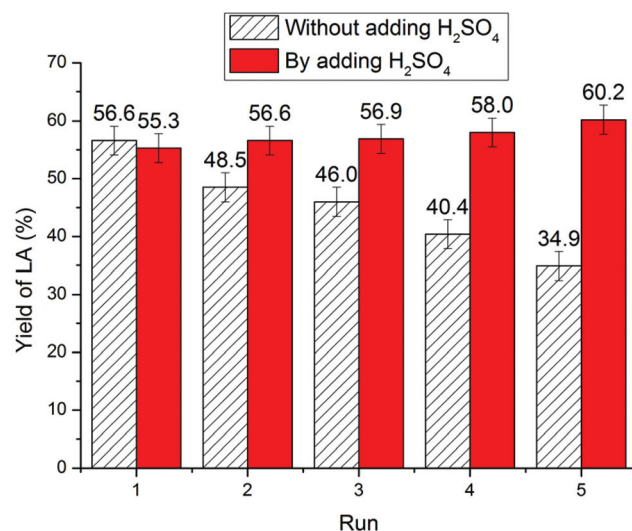


Fig. 9 The reuse of IL for chitin feedstock. Figure reproduced from ref. 63 with kind permission from The Royal Society of Chemistry.

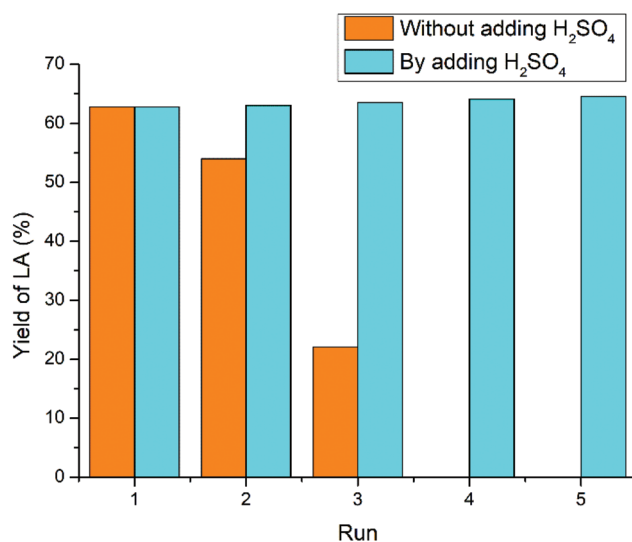


Fig. 10 The reuse of IL for raw crab shells. Figure reproduced from ref. 64 with kind permission from the American Chemical Society.

matic decline in catalytic activity could be partly ascribed to  $\text{NH}_3$  elimination during the conversion of raw crab shells, whereas  $\text{NH}_4^+$  was also detectable similar to our previous research on chitosan and chitin.<sup>61,63</sup> Besides, the  $\text{CaCO}_3$  component in the raw crab shells also consumes 1 equivalent of acidic IL, as  $\text{CO}_2$  bubbles were observed immediately once acidic IL was added to the crab shells. Hence, both deamination and the  $\text{CaCO}_3$  component accounted for the more dramatic decline in the acidity during recycling of raw crab shells compared with chitin feedstock. To offset this acidity loss, 1 equivalent of  $\text{H}_2\text{SO}_4$  corresponding to chitin and  $\text{CaCO}_3$  components was added to the reused IL and then the LA yield remained stable over five times.<sup>64</sup>

## 6. Comparison of different marine biomass

In order to demonstrate the different performance of various marine biomass (*i.e.*, chitosan, chitin, and crustacean shells), the same product model should be adopted. To date, there is only limited research on HMF and LA available to discuss.

### 6.1 HMF

With HMF product as the model, different performance of chitosan and chitin could be compared. Zang and co-workers used [Hmim]HSO<sub>4</sub> to hydrolyze chitosan and chitin at 180 °C for 5 h, leading to a HMF yield of 29.5 and 19.3%, respectively (Table 1, entries 3 and 9).<sup>57</sup>

With DMSO/H<sub>2</sub>O mixture as the solvent instead of water itself,<sup>58</sup> owing to the suppression of humin by-products, the conversion yields of chitosan and chitin to HMF were improved to 34.7% and 25.7%, respectively, by [Hmim]HSO<sub>4</sub> catalysis at 180 °C for 6 h (Table 1, entries 4 and 10). Both the aforementioned trends of higher HMF yields from chitosan than chitin indicated that efficient conversion of chitin is more difficult than that of chitosan under the same reaction conditions. Certainly, the optimum reaction conditions for chitosan and chitin should vary, which need to be optimized independently.

### 6.2 LA

Furthermore, with LA product as the model, the different performance of chitosan, chitin, and crustacean shells could be compared, whereas the reaction conditions have been optimized independently. The conversion yield of chitosan feedstock to LA was significantly increased to 64% by [C<sub>3</sub>SO<sub>3</sub>Hmim]HSO<sub>4</sub> catalysis at 170 °C for 5 h,<sup>61</sup> whereas higher temperature at 180 °C for 5 h promotes the formation of humins and causes the LA yield to decrease. This could be understood since the activation energy of humins is relatively higher than that of LA.

For chitin feedstock, through optimization of reaction conditions, 67.0% yield of LA was achieved with [C<sub>3</sub>SO<sub>3</sub>Hmim]HSO<sub>4</sub> as the catalyst at 180 °C for 5 h.<sup>63</sup> At 170 °C which is the optimum temperature for chitosan, chitin conversion to LA was incomplete, verifying that chitin conversion is more difficult than that of chitosan. This could be ascribed to the stronger hydrogen bonding network in chitin than chitosan.

For feedstock of crustacean shells such as crab shells, the yield of LA could be improved to 77.9% at 180 °C for 5 h by [C<sub>3</sub>SO<sub>3</sub>Hmim]HSO<sub>4</sub> catalysis.<sup>64</sup> 1.5 g of [C<sub>3</sub>SO<sub>3</sub>Hmim]HSO<sub>4</sub> was required for 250 mg of crab shells due to higher acid consumption by both deamination and the CaCO<sub>3</sub> component, while only 1.0 g of [C<sub>3</sub>SO<sub>3</sub>Hmim]HSO<sub>4</sub> was needed for 250 mg of chitin feedstock. Except the amount of [C<sub>3</sub>SO<sub>3</sub>Hmim]HSO<sub>4</sub>, the conversion difficulty of crab shells and chitin is similar (Table 1, entries 7, 11 and 12).

In addition to the effect of reaction conditions discussed as above, the different structural effects of ILs for each type of

marine biomass have been summarized, with respect to acidity and hydrogen bonding ability, as described in Sections 2.4, 3.4, and 4.1. Moreover, the different recyclability of ILs for each type of marine biomass have been discussed in Section 5. Therefore, it can be seen that different marine biomass perform differently to achieve the same product, with respect to reaction conditions, and structural effect and recyclability of ILs.

## 7. Conclusions and outlook

In comparison with the significant achievements of ILs in the conversion of lignocellulosic biomass, the methodological developments of ILs in marine biomass have been rather limited due to the higher structural complexity of marine biomass. In this review, the early applications of acidic ILs as catalysts in the conversion of marine biomass, including chitosan, chitin, and crustacean shells have been reviewed according to the order of feedstock from simple to complex. A variety of high value-added chemicals, *e.g.*, chitosan oligomers, sugars, 3A5AF, HMF and LA, have been produced. The different characteristics of ILs for each type of marine biomass have been summarized and compared with lignocellulosic biomass, with respect to acidity, hydrogen bonding ability and recyclability, demonstrating the structural effect of marine biomass on their conversion. In addition, as derived through comparison of different marine biomass, the conversion difficulty of crab shells and chitin is similar, which is much higher than that of chitosan. The review is deemed to provide in-depth insights into how to improve the conversion efficiency of marine biomass towards the target product by the catalysis of ILs. It can be foreseen that more exciting applications of ILs in the conversion of marine biomass are on the way to advance the marine-based green chemistry. There are many challenges and opportunities, and we would like to highlight some as follows:

(1) According to the special structural features of different marine biomass, comprehensive research on rational design of the IL structures should be conducted to efficiently convert marine biomass into specific chemical products.

(2) The network of downstream chemicals starting from marine biomass catalysed by ILs should be enlarged. More brand-new chemical routes await to be established, such as those of nitrogen-containing chemical products.

(3) In-depth mechanistic understanding on the conversion of marine biomass is required, *i.e.*, the mechanism of deamination, the formation of humin by-products, *etc.* which could in turn help to design the IL catalyst structures and develop new chemical routes.

(4) Highly efficient post-treatment after the conversion is necessary for practical applications. More innovative and environmentally benign technologies need to be developed to separate the chemical products and reuse the ILs simultaneously.

(5) Conversion of the raw crustacean shells, *e.g.*, crab and shrimp shells, requires more attention. The high-value utiliz-



ation of the other components of  $\text{CaCO}_3$  and protein needs to be explored. The integrated route of all components could be developed by taking advantage of the natural structures of the crustacean shells.

(6) Industrial applications of producing chemicals from marine biomass are the longstanding goals in this new but promising field. The final utility of a chemical route will mainly depend on the feedstock and processing cost. This involves tremendous efforts from fundamental research to process integration in the future.

## Conflicts of interest

There are no conflicts to declare.

## Acknowledgements

This work was supported by the Program of Higher-level Talents of IMU (10000-21311201/145), and the Fujian Provincial Key Lab of Coastal Basin Environment (S1-KF2008).

## Notes and references

- G. W. Huber, J. N. Chheda, C. J. Barrett and J. A. Dumesic, *Science*, 2005, **308**, 1446–1450.
- G. W. Huber, S. Iborra and A. Corma, *Chem. Rev.*, 2006, **106**, 4044–4098.
- J. N. Chheda, G. W. Huber and J. A. Dumesic, *Angew. Chem., Int. Ed.*, 2007, **46**, 7164–7183.
- A. Corma, S. Iborra and A. Velty, *Chem. Rev.*, 2007, **107**, 2411–2502.
- J. B. Binder and R. T. Raines, *J. Am. Chem. Soc.*, 2009, **131**, 1979–1985.
- J. C. Serrano-Ruiz, R. Luque and A. Sepulveda-Escribano, *Chem. Soc. Rev.*, 2011, **40**, 5266–5281.
- C.-H. Zhou, X. Xia, C.-X. Lin, D.-S. Tong and J. Beltramini, *Chem. Soc. Rev.*, 2011, **40**, 5588–5617.
- D. M. Alonso, S. G. Wettstein and J. A. Dumesic, *Chem. Soc. Rev.*, 2012, **41**, 8075–8098.
- P. Gallezot, *Chem. Soc. Rev.*, 2012, **41**, 1538–1558.
- D. M. Alonso, S. G. Wettstein, M. A. Mellmer, E. I. Gurbuz and J. A. Dumesic, *Energy Environ. Sci.*, 2013, **6**, 76–80.
- E. I. Gurbuz, J. M. R. Gallo, D. M. Alonso, S. G. Wettstein, W. Y. Lim and J. A. Dumesic, *Angew. Chem., Int. Ed.*, 2013, **52**, 1270–1274.
- M. Besson, P. Gallezot and C. Pinel, *Chem. Rev.*, 2014, **114**, 1827–1870.
- K. Barta and P. C. Ford, *Acc. Chem. Res.*, 2014, **47**, 1503–1512.
- J. Q. Bond, A. A. Upadhye, H. Olcay, G. A. Tompsett, J. Jae, R. Xing, D. M. Alonso, D. Wang, T. Y. Zhang, R. Kumar, A. Foster, S. M. Sen, C. T. Maravelias, R. Malina, S. R. H. Barrett, R. Lobo, C. E. Wyman, J. A. Dumesic and G. W. Huber, *Energy Environ. Sci.*, 2014, **7**, 1500–1523.
- L. T. Mika, E. Cséfalvay and A. Németh, *Chem. Rev.*, 2018, **118**, 505–613.
- A. J. Ragauskas, C. K. Williams, B. H. Davison, G. Britovsek, J. Cairney, C. A. Eckert, W. J. Frederick Jr., J. P. Hallett, D. J. Leak, C. L. Liotta, J. R. Mielenz, R. Murphy, R. Templer and T. Tschaplinski, *Science*, 2006, **311**, 484–489.
- J. B. Binder and R. T. Raines, *Proc. Natl. Acad. Sci. U. S. A.*, 2010, **107**, 4516–4521.
- J. S. Luterbacher, J. M. Rand, D. M. Alonso, J. Han, J. T. Youngquist, C. T. Maravelias, B. F. Pfleger and J. A. Dumesic, *Science*, 2014, **343**, 277–280.
- Q. Xia, Z. Chen, Y. Shao, X. Gong, H. Wang, X. Liu, S. F. Parker, X. Han, S. Yang and Y. Wang, *Nat. Commun.*, 2016, **7**, 11162.
- N. Yan and X. Chen, *Nature*, 2015, **524**, 155–157.
- T. Maschmeyer, R. Luque and M. Selva, *Chem. Soc. Rev.*, 2020, **49**, 4527–4563.
- F. M. Kerton, Y. Liu, K. W. Omari and K. Hawboldt, *Green Chem.*, 2013, **15**, 860–871.
- M. Mascal and E. B. Nikitin, *ChemSusChem*, 2009, **2**, 859–861.
- M. W. Drover, K. W. Omari, J. N. Murphy and F. M. Kerton, *RSC Adv.*, 2012, **2**, 4642–4644.
- Y. Wang, C. M. Pedersen, T. Deng, Y. Qiao and X. Hou, *Bioresour. Technol.*, 2013, **143**, 384–390.
- X. Gao, X. Chen, J. Zhang, W. Guo, F. Jin and N. Yan, *ACS Sustainable Chem. Eng.*, 2016, **4**, 3912–3920.
- X. Chen, Y. Gao, L. Wang, H. Chen and N. Yan, *ChemPlusChem*, 2015, **80**, 1565–1572.
- M. Yabushita, H. Kobayashi, K. Kuroki, S. Ito and A. Fukuoka, *ChemSusChem*, 2015, **8**, 3760–3763.
- H. Kobayashi, K. Techikawara and A. Fukuoka, *Green Chem.*, 2017, **19**, 3350–3356.
- G. Margoutidis, V. H. Parsons, C. S. Bottaro, N. Yan and F. M. Kerton, *ACS Sustainable Chem. Eng.*, 2018, **6**, 1662–1669.
- E. Husson, C. Hadad, G. Huet, S. Laclef, D. Lesur, V. Lambertyn, A. Jamali, S. Gottis, C. Sarazin and A. N. V. Nhien, *Green Chem.*, 2017, **19**, 4122–4131.
- X. Chen, H. Yang, Z. Zhong and N. Yan, *Green Chem.*, 2017, **19**, 2783–2792.
- X. Chen, H. Yang and N. Yan, *Chem. – Eur. J.*, 2016, **22**, 13402–13421.
- M. J. Hulsey, H. Yang and N. Yan, *ACS Sustainable Chem. Eng.*, 2018, **6**, 5694–5707.
- R. D. Rogers and K. R. Seddon, *Science*, 2003, **302**, 792–793.
- N. V. Plechkova and K. R. Seddon, *Chem. Soc. Rev.*, 2008, **37**, 123–150.
- J. P. Hallett and T. Welton, *Chem. Rev.*, 2011, **111**, 3508–3576.
- R. P. Swatloski, S. K. Spear, J. D. Holbrey and R. D. Rogers, *J. Am. Chem. Soc.*, 2002, **124**, 4974–4975.
- A. Brandt, J. Grasvik, J. P. Hallett and T. Welton, *Green Chem.*, 2013, **15**, 550–583.

- 40 C. Li and Z. K. Zhao, *Adv. Synth. Catal.*, 2007, **349**, 1847–1850.
- 41 H. Zhao, J. E. Holladay, H. Brown and Z. C. Zhang, *Science*, 2007, **316**, 1597–1600.
- 42 R. Rinaldi, R. Palkovits and F. Schueth, *Angew. Chem., Int. Ed.*, 2008, **47**, 8047–8050.
- 43 A. Pinkert, K. N. Marsh, S. Pang and M. P. Staiger, *Chem. Rev.*, 2009, **109**, 6712–6728.
- 44 M. E. Zakrzewska, E. Bogel-Lukasik and R. Bogel-Lukasik, *Chem. Rev.*, 2011, **111**, 397–417.
- 45 H. Ren, Y. Zhou and L. Liu, *Bioresour. Technol.*, 2013, **129**, 616–619.
- 46 A. M. da Costa Lopes and R. Bogel-Lukasik, *ChemSusChem*, 2015, **8**, 947–965.
- 47 A. S. Amarasekara, *Chem. Rev.*, 2016, **116**, 6133–6183.
- 48 Z. Zhang, J. Song and B. Han, *Chem. Rev.*, 2017, **117**, 6834–6880.
- 49 H. Xie, S. Zhang and S. Li, *Green Chem.*, 2006, **8**, 630–633.
- 50 Y. Wu, T. Sasaki, S. Irie and K. Sakurai, *Polymer*, 2008, **49**, 2321–2327.
- 51 Y. Qin, X. Lu, N. Sun and R. D. Rogers, *Green Chem.*, 2010, **12**, 968–971.
- 52 J. L. Shamshina, *Green Chem.*, 2019, **21**, 3974–3993.
- 53 J. L. Shamshina, P. Berton and R. D. Rogers, *ACS Sustainable Chem. Eng.*, 2019, **7**, 6444–6457.
- 54 Z. Zhang, C. Li, Q. Wang and Z. K. Zhao, *Carbohydr. Polym.*, 2009, **78**, 685–689.
- 55 A. Pandit, L. Khare, P. Ganatra, R. Jain and P. Dandekar, *Carbohydr. Polym.*, 2021, **260**, 117828.
- 56 Q. Chen, W. J. Xiao, L. L. Zhou, T. H. Wu and Y. Wu, *Polym. Degrad. Stab.*, 2012, **97**, 49–53.
- 57 M. Li, H. Zang, J. Feng, Q. Yan, N. Yu, X. Shi and B. Cheng, *Polym. Degrad. Stab.*, 2015, **121**, 331–339.
- 58 H. J. Zang, S. B. Yu, P. F. Yu, H. Y. Ding, Y. N. Du, Y. C. Yang and Y. W. Zhang, *Carbohydr. Res.*, 2017, **442**, 1–8.
- 59 Y. Jiang, H. J. Zang, S. Han, B. Yan, S. B. Yu and B. W. Cheng, *RSC Adv.*, 2016, **6**, 103774–103781.
- 60 M. C. Zhang, H. J. Zang, B. Ma, X. L. Zhang, R. R. Xie and B. W. Cheng, *ChemistrySelect*, 2017, **2**, 10323–10328.
- 61 W. Hou, L. Liu and H. Shen, *Carbohydr. Polym.*, 2018, **195**, 267–274.
- 62 W. M. Reichert, A. Mirjafari, J. H. Davis Jr., T. Goodie, N. G. Williams, V. Ho, M. Yoder and M. La, in *Ionic Liquids: Science and Applications*, ed. A. E. Visser, N. J. Bridges and R. D. Rogers, 2012, vol. 1117, pp. 189–198.
- 63 W. Hou, Q. Zhao and L. Liu, *Green Chem.*, 2020, **22**, 62–70.
- 64 Q. Zhao and L. Liu, *ACS Sustainable Chem. Eng.*, 2021, **9**, 1762–1771.
- 65 Q. Chen, A. Xu, Z. Li, J. Wang and S. Zhang, *Green Chem.*, 2011, **13**, 3446–3452.
- 66 Y. Jiang, H. Zang, S. Han, B. Yan, S. Yu and B. Cheng, *RSC Adv.*, 2016, **6**, 103774–103781.
- 67 H. Ren, B. Girisuta, Y. Zhou and L. Liu, *Carbohydr. Polym.*, 2015, **117**, 569–576.
- 68 L. Liu, Z. Li, W. Hou and H. Shen, *Carbohydr. Polym.*, 2018, **181**, 778–784.
- 69 X. Zhao, A. Kong, Y. Hou, C. Shan, H. Ding and Y. Shan, *Carbohydr. Res.*, 2009, **344**, 2010–2013.
- 70 L. Li, B. Yuan, S. W. Liu, S. T. Yu, C. X. Xie, F. S. Liu and L. J. Shan, *J. Polym. Environ.*, 2012, **20**, 388–394.
- 71 K. W. Omari, J. E. Besaw and F. M. Kerton, *Green Chem.*, 2012, **14**, 1480–1487.
- 72 S. E. Davis, B. N. Zope and R. J. Davis, *Green Chem.*, 2012, **14**, 143–147.
- 73 E. Hayashi, Y. Yamaguchi, K. Kamata, N. Tsunoda, Y. Kumagai, F. Oba and M. Hara, *J. Am. Chem. Soc.*, 2019, **141**, 890–900.
- 74 B. Saha, C. M. Bohn and M. M. Abu-Omar, *ChemSusChem*, 2014, **7**, 3095–3101.
- 75 W. Guo, H. Liu, S. Zhang, H. Han, H. Liu, T. Jiang, B. Han and T. Wu, *Green Chem.*, 2016, **18**, 6222–6228.
- 76 R. Fang, R. Luque and Y. Li, *Green Chem.*, 2016, **18**, 3152–3157.
- 77 Z. Zhang and G. W. Huber, *Chem. Soc. Rev.*, 2018, **47**, 1351–1390.
- 78 B. Girisuta, L. P. B. M. Janssen and H. J. Heeres, *Green Chem.*, 2006, **8**, 701–709.
- 79 R.-J. van Putten, J. C. van der Waal, E. de Jong, C. B. Rasrendra, H. J. Heeres and J. G. de Vries, *Chem. Rev.*, 2013, **113**, 1499–1597.
- 80 J. B. Binder, A. V. Cefali, J. J. Blank and R. T. Raines, *Energy Environ. Sci.*, 2010, **3**, 765–771.
- 81 B. Kim, J. Jeong, D. Lee, S. Kim, H. J. Yoon, Y. S. Lee and J. K. Cho, *Green Chem.*, 2011, **13**, 1503–1506.
- 82 S.-B. Lee and G.-T. Jeong, *Appl. Biochem. Biotechnol.*, 2015, **176**, 1151–1161.
- 83 S. Yu, H. Zang, S. Chen, Y. Jiang, B. Yan and B. Cheng, *Polym. Degrad. Stab.*, 2016, **134**, 105–114.
- 84 D. W. Rackemann and W. O. S. Doherty, *Biofuels, Bioprod. Biorefin.*, 2011, **5**, 198–214.
- 85 S. M. Sen, D. M. Alonso, S. G. Wettstein, E. I. Gurbuz, C. A. Henao, J. A. Dumesic and C. T. Maravelias, *Energy Environ. Sci.*, 2012, **5**, 9690–9697.
- 86 M. J. Climent, A. Corma and S. Iborra, *Green Chem.*, 2014, **16**, 516–547.
- 87 A. Morone, M. Apte and R. A. Pandey, *Renewable Sustainable Energy Rev.*, 2015, **51**, 548–565.
- 88 F. D. Pileidis and M.-M. Titirici, *ChemSusChem*, 2016, **9**, 562–582.
- 89 Y. Shao, K. Sun, Q. Li, Q. Liu, S. Zhang, Q. Liu, G. Hu and X. Hu, *Green Chem.*, 2019, **21**, 4499–4511.
- 90 H.-J. Feng, X.-C. Li, H. Qian, Y.-F. Zhang, D.-H. Zhang, D. Zhao, S.-G. Hong and N. Zhang, *Green Chem.*, 2019, **21**, 1743–1756.
- 91 R. Weingarten, W. C. Conner and G. W. Huber, *Energy Environ. Sci.*, 2012, **5**, 7559–7574.
- 92 S. G. Wettstein, D. M. Alonso, Y. X. Chong and J. A. Dumesic, *Energy Environ. Sci.*, 2012, **5**, 8199–8203.
- 93 J. J. Bozell, *Science*, 2010, **329**, 522–523.

- 94 S. Van de Vyver, J. Thomas, J. Geboers, S. Keyzer, M. Smet, W. Dehaen, P. A. Jacobs and B. F. Sels, *Energy Environ. Sci.*, 2011, **4**, 3601–3610.
- 95 J. Q. Bond, D. M. Alonso, D. Wang, R. M. West and J. A. Dumesic, *Science*, 2010, **327**, 1110–1114.
- 96 R. A. Sheldon, *Green Chem.*, 2014, **16**, 950–963.
- 97 Á. Szabolcs, M. Molnár, G. Dibó and L. T. Mika, *Green Chem.*, 2013, **15**, 439–445.
- 98 S. J. Dee and A. T. Bell, *ChemSusChem*, 2011, **4**, 1166–1173.
- 99 I. van Zandvoort, Y. H. Wang, C. B. Rasrendra, E. R. H. van Eck, P. C. A. Bruijninx, H. J. Heeres and B. M. Weckhuysen, *ChemSusChem*, 2013, **6**, 1745–1758.
- 100 X. Fu, J. Dai, X. Guo, J. Tang, L. Zhu and C. Hu, *Green Chem.*, 2017, **19**, 3334–3343.
- 101 Z. Cheng, J. L. Everhart, G. Tsilomelekis, V. Nikolakis, B. Saha and D. G. Vlachos, *Green Chem.*, 2018, **20**, 997–1006.
- 102 V. Maruani, S. Narayanin-Richenapin, E. Framery and B. Andrioletti, *ACS Sustainable Chem. Eng.*, 2018, **6**, 13487–13493.
- 103 Z. Cheng, K. A. Goulas, N. Q. Rodriguez, B. Saha and D. G. Vlachos, *Green Chem.*, 2020, **22**, 2301–2309.
- 104 A. Sangregorio, A. Muralidhara, N. Guigo, L. G. Thygesen, G. Marlaire, C. Angelici, E. de Jong and N. Sbirrazzuoli, *Green Chem.*, 2020, **22**, 2786–2798.
- 105 H. Shen, H. Shan and L. Liu, *ChemSusChem*, 2020, **13**, 513–519.
- 106 R. C. Remsing, R. P. Swatloski, R. D. Rogers and G. Moyna, *Chem. Commun.*, 2006, 1271–1273.
- 107 A. Xu, J. Wang and H. Wang, *Green Chem.*, 2010, **12**, 268–275.
- 108 H. Wang, G. Gurau and R. D. Rogers, *Chem. Soc. Rev.*, 2012, **41**, 1519–1537.
- 109 P. Sikorski, R. Hori and M. Wada, *Biomacromolecules*, 2009, **10**, 1100–1105.
- 110 P. S. Barber, C. S. Griggs, G. Gurau, Z. Liu, S. Li, Z. Li, X. Lu, S. Zhang and R. D. Rogers, *Angew. Chem., Int. Ed.*, 2013, **52**, 12350–12353.
- 111 M. Shimo, M. Abe and H. Ohno, *ACS Sustainable Chem. Eng.*, 2016, **4**, 3722–3727.
- 112 T. Uto, S. Idenoue, K. Yamamoto and J.-i. Kadokawa, *Phys. Chem. Chem. Phys.*, 2018, **20**, 20669–20677.
- 113 A. C. Cole, J. L. Jensen, I. Ntai, K. L. T. Tran, K. J. Weaver, D. C. Forbes and J. H. Davis, *J. Am. Chem. Soc.*, 2002, **124**, 5962–5963.
- 114 K. W. Omari, L. Dodot and F. M. Kerton, *ChemSusChem*, 2012, **5**, 1767–1772.
- 115 X. Chen, S. L. Chew, F. M. Kerton and N. Yan, *Green Chem.*, 2014, **16**, 2204–2212.
- 116 X. Chen, Y. Liu, F. M. Kerton and N. Yan, *RSC Adv.*, 2015, **5**, 20073–20080.
- 117 T. Setoguchi, T. Kato, K. Yamamoto and J.-i. Kadokawa, *Int. J. Biol. Macromol.*, 2012, **50**, 861–864.
- 118 H. K. No, S. P. Meyers and K. S. Lee, *J. Agric. Food Chem.*, 1989, **37**, 575–579.
- 119 F. Shahidi and J. Synowiecki, *J. Agric. Food Chem.*, 1991, **39**, 1527–1532.
- 120 M. Boric, H. Puliyalil, U. Novak and B. Likozar, *Green Chem.*, 2018, **20**, 1199–1204.
- 121 P. Beaney, J. Lizardi-Mendoza and M. Healy, *J. Chem. Technol. Biotechnol.*, 2005, **80**, 145–150.
- 122 P. S. Barber, C. S. Griggs, J. R. Bonner and R. D. Rogers, *Green Chem.*, 2013, **15**, 601–607.
- 123 J. L. Shamshina, G. Gurau, L. E. Block, L. K. Hansen, C. Dingee, A. Walters and R. D. Rogers, *J. Mater. Chem. B*, 2014, **2**, 3924–3936.
- 124 X. Shen, J. L. Shamshina, P. Berton, J. Bandomir, H. Wang, G. Gurau and R. D. Rogers, *ACS Sustainable Chem. Eng.*, 2016, **4**, 471–480.
- 125 C. King, J. L. Shamshina, G. Gurau, P. Berton, N. F. A. F. Khan and R. D. Rogers, *Green Chem.*, 2017, **19**, 117–126.
- 126 J. L. Shamshina, P. S. Barber, G. Gurau, C. S. Griggs and R. D. Rogers, *ACS Sustainable Chem. Eng.*, 2016, **4**, 6072–6081.
- 127 M. Feng, X. Lu, L. Wang, J. Zhang, S. Yang, C. Shi, Q. Zhou and S. Zhang, *ACS Sustainable Chem. Eng.*, 2019, **7**, 11990–11998.
- 128 X. Ma, G. Gozaydin, H. Yang, W. Ning, X. Han, N. Y. Poon, H. Liang, N. Yan and K. Zhou, *Proc. Natl. Acad. Sci. U. S. A.*, 2020, **117**, 7719–7728.
- 129 S. Hu, Z. Zhang, Y. Zhou, J. Song, H. Fan and B. Han, *Green Chem.*, 2009, **11**, 873–877.
- 130 J. Song, H. Fan, J. Ma and B. Han, *Green Chem.*, 2013, **15**, 2619–2635.
- 131 L. Wu, J. Song, B. Zhang, B. Zhou, H. Zhou, H. Fan, Y. Yang and B. Han, *Green Chem.*, 2014, **16**, 3935–3941.
- 132 X. Sun, Z. Liu, Z. Xue, Y. Zhang and T. Mu, *Green Chem.*, 2015, **17**, 2719–2722.
- 133 L. C. Nhien, L. Nguyen Van Duc, S. Kim and M. Leet, *Ind. Eng. Chem. Res.*, 2016, **55**, 5180–5189.